Nucl. Sci. and Tech., Vol.8, No. 2 (2018), pp. 19-26

Nuclear Science and Technology

Journal homepage: https://jnst.vn/index.php/nst

Application of correlation pattern recognition technique for neutron–gamma discrimination in the EJ-301 liquid scintillation detector

Phan Van Chuan[1*], Truong Van Minh[2], Bui Thanh Trung[3], Nguyen Thi Phuc[1], Tran Ngọc Dieu Quynh[1]

[1]*Dalat University, 01 Phu Dong ThienVuong, Dalat, Lamdong, Vietnam*
[2]*Dongnai University, 04 Le Quy Don, Bienhoa, Dongnai, Vietnam*
[3]*MSc Student of Department of Postgraduate Studies, Dalat University, 01 Phu Dong Thien Vuong, Dalat, Lamdong*
[*]*Corresponding author email: chuanpv@dlu.edu.vn*

Abstract: The ability to distinguish between neutrons and gamma-rays is important in the fast - neutron detection, especially when using the *scintillation detector*. A dual correlation pattern recognition (DCPR) method that was based on the correlation pattern recognition technique has been developed for classification of neutron/gamma events from a *scintillation* detector. In this study, an EJ-301 liquid scintillation (EJ301) detector was used to detect neutrons and gamma-rays from the ^{60}Co and ^{252}Cf sources; the EJ301 detector's pulses were digitized by a digital oscilloscope and its pulse-shape discriminant (PSD) parameters were calculated by the correlation pattern recognition (CPR) method with the reference neutron and gamma-ray pulses. The digital charge integration (DCI) method was also used as a reference-method for comparison with DCPR method. The figure-of-merit (FOM) values which were calculated in the 50 ÷ 1100 keV electron equivalent (keVee) region showed that the DCPR method outperformed the DCI method. The FOMs of 50, 420 and 1000 keVee thresholds of DCPR method are 0.82 , 2.2 and 1.62, which are 1.55, 1.77, and 1.1 times greater than the DCI method, respectively.

Keywords: *Correlation pattern recognition method, EJ301 detector, pulse shape discrimination (PSD).*

I. INTRODUCTION

The EJ-301 liquid scintillator has been widely used for detection of both neutrons and gamma-rays [1, 2]. The scintillation-light output of the EJ-301 display both fast and slow decay components, which depend on either neutron or gamma-ray of excitation radiations [2, 3, 4, 5]. By coupling the scintillator EJ-301 cell to a photomultiplier tube (PMT), the light can be collected and converted into a voltage pulse, allowing for data acquisition/processing. These pulses are generated in different-shapes between neutron and gamma-ray, so neutron and gamma-ray can be identified by the pulse shape discrimination (PSD) techniques [1, 3-8]. Many PSD methods have been developed for fast-neutron detectors, however, the charge comparison (CC) [4] and the zero crossing (ZC) [3, 4, 6, 9] methods are the most commonly used in analogue systems.

Recently, the fast analog-to-digital converters (ADCs), field programmable gate array (FPGA), and digital signal processing (DSP) technology have been applied in neutron/gamma PSD systems that are supposed to result in more powerful discrimination qualities. Although many publications on PSD, for example, digital charge integration (DCI) [4, 6-8, 10, 11], frequency domain analysis [5], pulse gradient analysis [12], correlation pattern

https://doi.org/10.53747/jnst.v8i2.87
Received 06 June 2018, accepted 16 August 2018

recognition (CPR) [13, 14], Zero crossing [8], threshold crossing time (TCT) [15], and curve fitting (CF) [13, 16], have been published, the separation between neutrons and gamma-rays is not good for the low-energy region (below 200 keVee). In the study of D. Takaku et al., 2011 (see [13]), the CPR method which was calculated with gamma reference pulse showed that the PSD ability of CPR method is better than the DCI and CF methods. Though, the PSD's ability in below the threshold of 700 keVee had not been investigated. The Question has been raised whether PSD's ability can be improved when combining CPR methods for both neutron and gamma reference pulse in the low-energy region.

In this study, a dual correlation pattern recognition (DCPR) method was developed to distinguish between neutrons and gamma-rays for a fast-neutron detector using the EJ-301 liquid scintillation (called EJ301 detector). Based on the correlation pattern recognition technique, the DCPR method used the set of pulses that were digitized by a digital oscilloscope with 11-bit resolution and sampling rate at 1 Giga sampling per second (GSPS). The programs for the DCPR and DCI methods were implemented in the MATLAB software and the FOMs were calculated by OriginLab software.

II. MATERIALS AND METHODS

A. Experimental setup

A EJ301 detector consists of a liquid scintillator container (cell), photo-multiplier tube (PMT), voltage divider, cover shield and preamplifier. The cell is left cylinder made of aluminum with 34-mm diameter and 60-mm length in size. A diagram of the experimental setup is shown in Fig. 1. The EJ301 detector was operated with negative biases of 1200V. The signals from the anode of the PMT is digitized by a digital oscilloscope (Tektronix DPO7254C) with 2.5 GHz bandwidth, 11-bits resolution equivalent and at a sampling rate of 1 GSPS.A neutron ^{252}Cf source (11.6 mCi) and gamma-ray sources (^{22}Na, ^{137}Cs and ^{60}Co) were used for energy calibration and assessment of neutron/gamma discrimination for the DCI and DCPR methods.In this measurement, the EJ301 detector was placed 1 cm away from the gamma-ray sources and 100 cm away from the ^{252}Cf source.

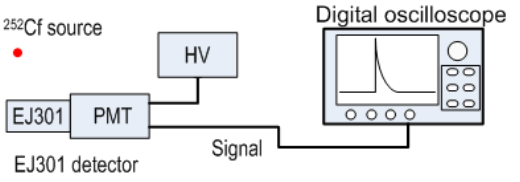

Fig. 1. Diagram of the experimental setup.

B. Pulse shape discrimination method

Approximately 100,000 pulses in the range from 50 to 1100 keVee that was divided into 10 thresholds and 200,000 pulses in the range from 50 to 1500 keVee were used to test this method. Each pulse was sampled consist of 360 samples which was started at a point in front of trigger-point and the baseline was calculated of 90 points in the pre-trigger range of pulses. The baseline was used in the DCI method in order to determine the digital integral to be more accurate.

Digital charge integration (DCI) method

The DCI method consist of integration techniques with digitized pulses was chosen for comparison with DCPR method, where each pulse was integrated twice, using two different ranges [6, 7, 8, 10, 11]. The typical neutron and gamma-ray pulses with the same amplitude are shown in the Fig. 2; the neutron pulses exhibit a larger decay time to the baseline, so the tail to total integral ratio of neutron pulses are greater than that of the gamma pulses and are used as a PSD parameter. The total integral is calculated for an entire pulse that begins at the trigger-point (t_1) to an optimized point of tail-pulse (t_3). The tail integral, meanwhile, is

calculated in range begins at a fixed position after peak-pulse (t_2) and also is extended to the last data point chosen in the total integral range (t_3). Surveys showed that the optimal PSD when t_2 is chosen at 40ns and t_3 is chosen at 210ns after the peak-pulse.

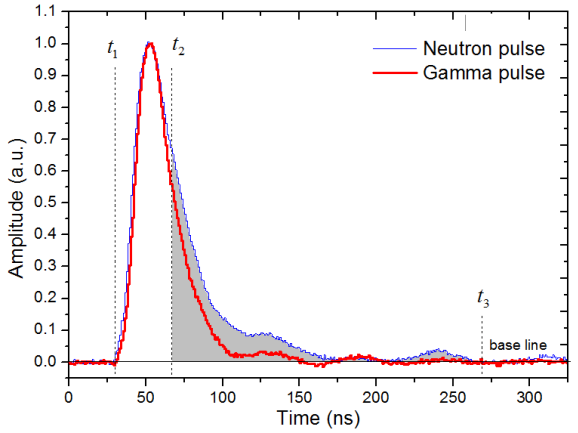

Fig. 2. Typical neutron and gamma-ray pulses in one sampling.

CPR method

The similarity (S) is used to recognize a pattern when a pattern can be expressed as a vector. In the CPR method, a measured pulse is regarded as an object vector X and a reference pulse is regarded as object vector Y. The reference pulse was averaged of thousands the gamma-ray pulses that were measured from the gamma-ray source (^{60}Co). A measured pulse is identified by calculating the scalar-product of X and Y vectors [5].

$$S = \frac{X.Y}{|X|.|Y|} = cos\theta \quad (1)$$

Where, X is vector of measured pulse; Y is vector of reference pulse; θ is the angle between X and Y vectors.

The PSD parameter is calculated by the correlation-angles in Eq. (2).

$$\theta = Acrcos\frac{\sum_{i=1}^{n} x_i.y_i}{\sqrt{\sum_{i=1}^{n} x_i^2}\sqrt{\sum_{i=1}^{n} y_i^2}} \quad (2)$$

Where, $\theta(rad)$ is the angle between the X and Y vectors; x_i and y_i are values of the i^{th} sampling of measured pulse and reference pulse, respectively.

Creating reference-pulses of neutron and gamma-ray

In order to obtain the reference-pulses of gamma-ray (RPG) and the reference-pulses of neutron (RPN), a large number of digitizing pulses from the ^{252}Cf source are identified by the DCI method. In this experiment, some of the pulses between the valley of two Gaussian distribution could not be identified as neutrons or gamma-rays, so the neutron and gamma pulses were defined within the range as shown in Fig. 3. The gamma-rays region was chosen between 0.05 and 0.15, while the neutron region was chosen between 0.19 and 0.31; however, this region may be different with another detector. In fact, the tail to total integral ratio of gamma-pileup pulses are similar to that of neutron pulses. To limit pile-up pulses, approximately 100,000 pulses which were measured from the ^{252}Cf source with the threshold of 100 keVee was used to calculate the RPG and RPN. Both RPN and RPG were calculated by Eq. (3), and were normalized to unity (see the Fig. 4).

$$y_i = \frac{1}{m}\sum_{k=1}^{n} h_k \quad (3)$$

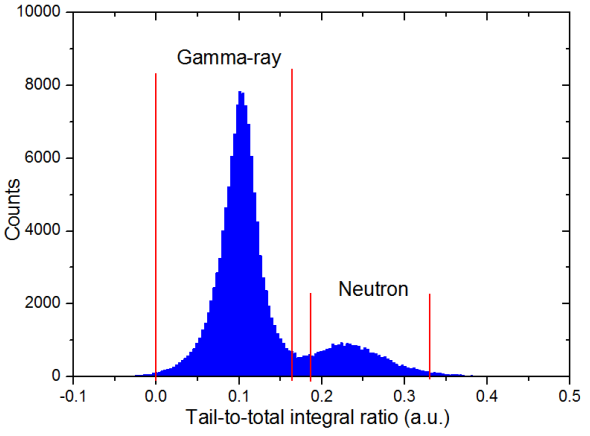

Fig. 3. The histogram of tail to total integral ratio of DCI method.

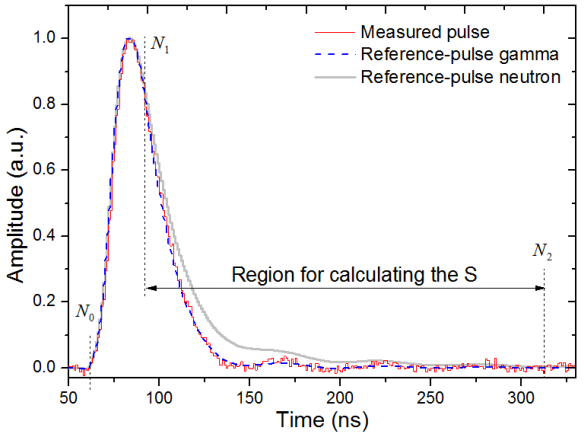

Fig. 4. The RPG and RPN were calculated by 100,000 pulses with the threshold of 100 keVee and the typically measured pulse (pulses normalized to the unit).

PSD optimization

In order to obtain the best neutron-gamma discrimination for the CPR method, many computing of correlation-angles were observed with the different start-position and length to calculate S. The survey showed that the optimal starting position is 5 ns after the peak-pulse and the length to calculate S is 210 ns. Therefore, the start position and length of the measured pulse was also calculated similarly for the reference-pulse.

DCPR method

In the DCPR method, a measured pulse was computed with both RPG and RPN by Eq. (2). Two PSD parameters the correlation-angle (θ_g) with the RPG and the correlation-angle (θ_n) with RPN) have obtained in this calculation. Two discrimination parameters (S_x and S_y) are computed by the Eq. (4)

$$\begin{cases} S_x = k_1\theta_g - k_2\theta_n \\ S_y = k_2\theta_g - k_1\theta_n \end{cases} \quad (4),$$

which are used to distinguish between neutrons and gamma-rays in the DCPR method. The k_1 and k_2 constants were chosen in order to obtain the optimal PSD parameter S_x; the k_1 and k_2 are chosen by $k_1 = cos\ (55^0)$ and $k_2 = cos\ (55^0)$.

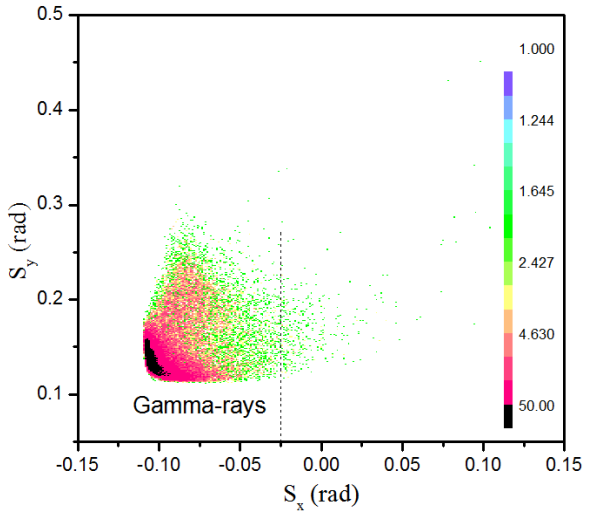

(a)

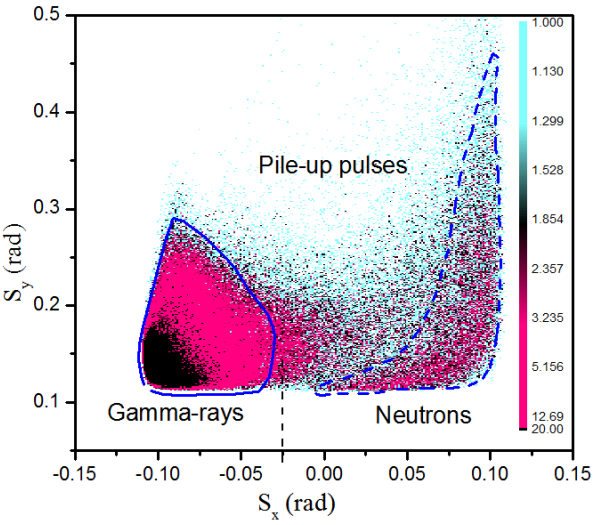

(b)

Fig. 5. The S_x-S_y scatterplot of the DCPR method for (a) ^{60}Co and (b) ^{252}Cf sources.

Fig. 5 shows the distributions of events as a function of the S_x and S_y parameters for two calculations with (a) the ^{60}Co source and (b) the ^{252}Cf source. The left-hand cluster of the dashed line is identified as gamma-ray events while the other side is identified as neutron events.

C. Analysis of pile-up events

The DCPR method identifies a pulse either neutron or gamma-rays based on S_x and S_y parameters, which also allows identification of pile-up pulses. In fact, the distortion-pulses and pileup-pulses are distributed between the neutrons cluster and the gamma-rays cluster in the S_xS_y-plane (Fig. 5 b). In order to determine the distribution of pileup-pulses in the S_xS_y-plane, a large number of pileup-pulses were generated by a program that used pure gamma-ray pulses. By adding two pulses, the pileup-pulses were generated when the second pulse appeared after the first pulse with random intervals. Fig. 6 shows the distribution of pileup-pulses, which was performed by the DCPR method; the boundary of pileup-pulses was defined by the Eq (5). The events which are above the curve (5) are considered as pileup; they, therefore, are eliminated in the DCPR method.

$$0.13 + 0.76x - 8.24x^2 - 372.92x^3 + 6660.72x^4 + 6714.66x^5 \quad (5)$$

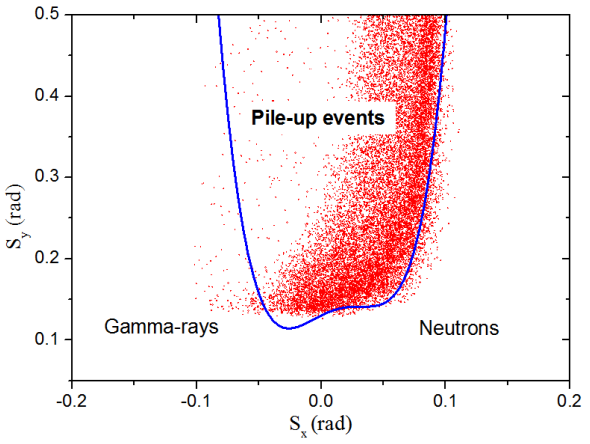

Fig. 6. The distribution of pileup-pulses in the S_xS_y-plane are calculated by the DCPR method.

D. Assessment of PSD performance

The performance of the PSD methods in this work is measured by their ability to accurately discriminate between pulse types, over a specified energy range, in a given measurement. These distributions of PSDs are usually obtained in the form of a Gaussian, which Gaussian fits maybe applied. The figure of merit (FOM) was used to evaluate the quantitative results of neutron/gamma discrimination, which was defined by Eq. (6) [1, 4-8,10,12,13,15, 17,18]. The higher FOM value is, the better PSD performs.

$$FOM = \frac{p_n - p_g}{FWHM_n + FWHM_g} \quad (6)$$

Where $p_n - p_g$ is the separation of two Gaussian fit peaks; $FWHM_n$ and $FWHM_g$ are the full-width-half-maximum of Gaussian fit peaks.

III. RESULTS AND DISCUSSION

Two measurements were conducted on the ^{252}Cf and ^{60}Co sources with the same EJ301 detector. The scatter-plot density of ^{252}Cf and ^{60}Co sources by the DCPR method which were calculated in MATLAB are shown in Fig. 7 (a) and (b), respectively. The discrimination parameter on the x-axis that was calculated by (4) used a separation threshold (with Sx = -0.75). The PSD-scatter plot with density and the histogram of the DCI method of the ^{225}Cf source are shown in Fig. 8 (a) and (b), respectively. The PSD-parameter on the Fig. 8 (a) was calculated by the tail to total integral ratio and the histogram on the Fig. 8 (b) was calculated for the PSD-parameter. The histograms of the DCPR method for ^{252}Cf and ^{60}Co sources are shown in Fig. 9 (a) and (b), respectively. The histogram in Fig. 9 (a) was fitted by the multi-peak Gaussian function and the FOM value was approximately 1.59. FOMs are shown in Fig. 10 as a function of energy thresholds. Each FOM value was calculated by the Gaussian fit in a dataset of 10,000 pulses for both the DCI method and the DCPR method.

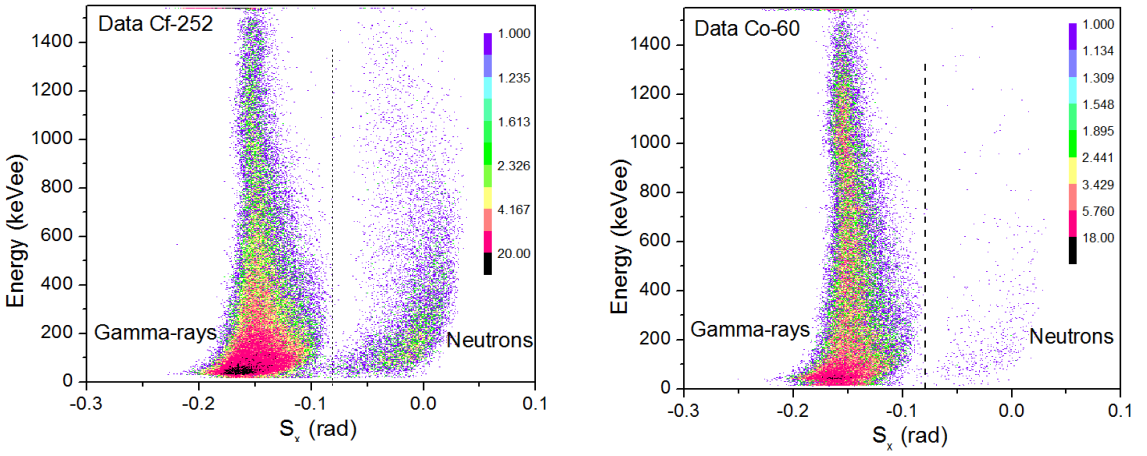

Fig. 7. The scatter plot of PSD parameters was implemented in the DCPR method.
(a) The ^{252}Cf source. (b) The ^{60}Co source.

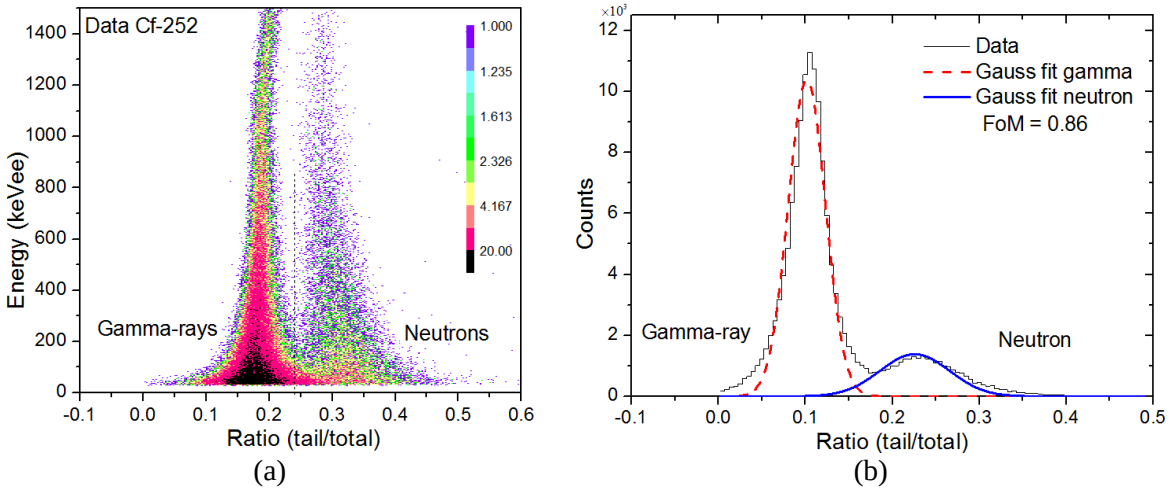

Fig. 8. The results of the DCI method were implemented in the ^{252}Cf source, using a 50 keVee threshold.
(a) The PSD scatter plots. (b) The histogram.

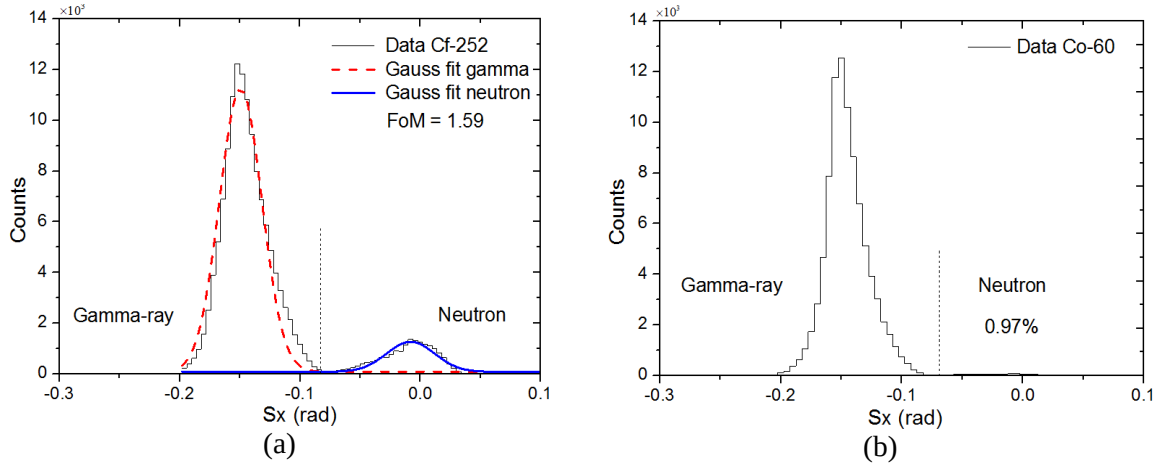

Fig. 9. Histogram obtained by the DCPR method with the threshold of 50 keVee.
(a) ^{252}Cf source. (b) ^{60}Co source.

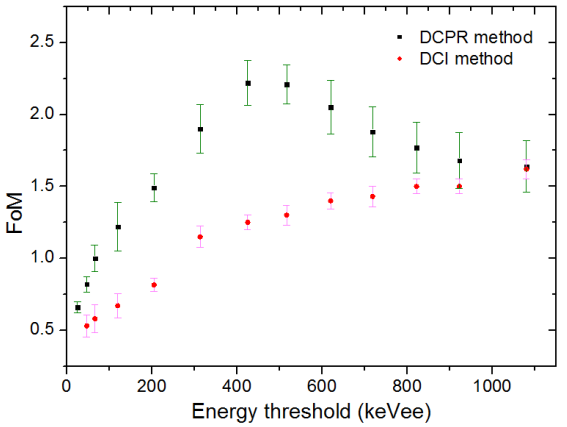

Fig. 10. FOMs were calculated as a function of energy thresholds in 50÷1100 keVee energy range.

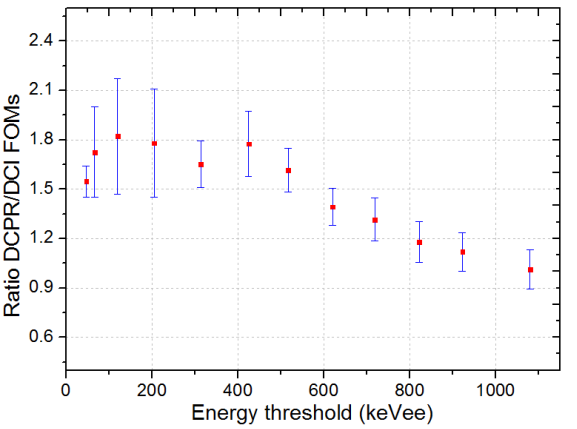

Fig. 11. The ratio of FOMs of the DCPR method to the DCI method.

A visual inspection of Fig. 7 (a) and Fig. 8 (a) shows that the DCPR method is more segregated than the DCI method, especially the below 200 keVee energy region. Using a separate-threshold in the histogram in Fig. 9 (a) and (b) shows that the data of ^{60}Co source were correctly identified by the DCPR method with approximately 99%. In fact, some gamma pile-up pulses are identified as neutron pulses in the DCPR method. The FOMs were calculated for the histograms in Fig. 8 (b) and Fig. 9 (a) for the 50 to 1500 keVee region were 1.59 for DCPR method and 0.86 for DCI method; it showed that FOM has improved of 1.85 times more than DCI method.

Based on the FOMs performances on Fig. 10, the DCPR method is better than the DCI method in the full-range survey. The DCPR method is increasing from 0.65 to 2.2 in the range of 30 - 420 keVee and smoothly dropping from 2.2 to 1.6 in the range of 420 - 1100 keVee, while the DCI method is continuously increased from 0.53 to 1.62 in range measured (50 - 1100 keVee). The ratio of FOM values between the DCPR method and the DCI method is shown Fig. 11; it has been shown that the ability to distinguish between neutrons and gamma-rays of the DCPR method is clearly improved in the region below 1000 keVee. While most other neutron/gamma PSD methods obtained bad results in the low region, the DCPR method has been improved in this region.

IV. CONCLUSIONS

A neutron-gamma PSD method has been developed based on the correlation pattern recognition method for the EJ301 detector. The ability to distinguish between neutron and gamma-ray of the DCPR method was clearly improved compared with that of DCI method in the region below 1000 keVee.

The algorithm of the DCPR method can be implemented on FPGA devices. Therefore, this method can be used in fast-neutron counting systems using PSD techniques for the EJ301 detector.

ACKNOWLEDGEMENT

The authors are thankful to the Nuclear Research Institute for providing necessary conditions during the implementation of this research.

REFERENCES

[1] S. D. Jastaniah, P. J. Sellin, "Digital pulse-shape algorithms for scintillation-based neutron detectors", *IEEE Trans. Nucl. Sci.* 49(4), 1824-1828, 2002.

[2]. <http://eljentechnology.com/products/liquid-scintillators/ej-301-ej-309>.

[3]. G. F. Knoll, "*Radiation Detection and Measurement"*, John Wiley & Sons, 2010.

[4]. A.Rahmat, L.R.Edward, F.S.David, "Development of a handheld device for simultaneous monitoring of fast neutrons and gamma rays", *IEEE Trans. Nucl. Sci.* 49(4), 1909-1913, 2002.

[5]. G. Liu, M. J. Joyce, X. Ma, M. D. Aspinall, "A digital method for the discrimination of neutrons and rays with organic scintillation detectors using frequency gradient analysis", *IEEE Trans. Nucl. Sci.* 57, 1682 – 1691, 2010.

[6]. C.S. Sosa, M. Flaska, S. A. Pozzi, "Comparison of analog and digital pulse-shape-discrimination systems", *Nucl. Inst. And Meth. A* 826, 72-79, 2016.

[7]. B.Wan, X. Y. Zhang, L. Chen, H. L. Ge, F. Ma, H. B. Zhang, Y. Q. Ju, Y. B. Zhang, Y.Y. Li, X.W. Xu, "Digital pulse shape discrimination methods for n - γ separation in an EJ-301 liquid scintillation detector", *Chinese Physics C.* Vol. 39, No. 11, 116201, 2015.

[8]. M. Nakhostin. P.M. Walker, "Application of digital zero-crossing technique for neutron–gamma discrimination in liquid organic scintillation detectors", *Nucl. Inst. and Meth. A* 621, 498501, 2010.

[9]. R. A. Winyard. J. E. Lutkin and G. W. Mcbeth, "Pulse Shape Discrimination In Inorganic And Organic Scintillators", *Nuclear Instruments And Methods 95, I4I--I53, I97I*.

[10]. C. Payne, P.J. Sellin, M. Ellis, K. Duroe, A. Jones, M. Joyce, G. Randall, R. Speller, "Neutron/gamma pulse shape discrimination in EJ-299-34 at high flux", *IEEE Nuclear Science Symposium and Medical Imaging Conference* (NSS/MIC), 2015.

[11]. F. Marek, F. Muhammad, D.Wentzloff, S.A.Pozzi, "Influence of sampling properties of fast-waveform digitizers on neutron – gamma-ray pulse-shape discrimination for organic scintillation detectors", *Nuclear Instruments and Methods in Physics Research* A 729, 456–462, 2013.

[12]. B. D. Mellow, M. D. Aspinall, R. O. Mackin, M. J. Joyce, and A. J. Peyton, "Digital discrimination of neutrons and γ-rays in liquid scintillators using pulse gradient analysis", *Nucl. Inst. and Meth. A* 578, 191 – 197, 2007.

[13]. D. Takaku, T. Oishi, and M. Baba, "Development of neutron-gamma discrimination technique using pattern-recognition method with digital signal processing", *Prog. Nucl. Sci. Technol.* 1, 210-213, 2011.

[14]. H. Sakai, A. Uritani, Y. Takenaka, C. Mori, T. Iguchi, "New pulse-shape analysis method with multi-shaping amplifers", *Nuclear Instruments and Methods in Physics Research* A 421, 316-321, 1999.

[15]. A. Moslem, P. Vaclav, C. Frantisek, M. Zdenek, M. Filip, J. Radioanal, "Quick algorithms for real-time discrimination of neutrons and gamma rays", *Nucl. Chem.* 303, 583599, 2015.

[16]. C. Guerrero, D. Cano Ott, M. O. Fernandez, E. R. Gonzalez, T. Martınez, D. Villamarın, "Analysis of the BC501A neutron detector signals using the true pulse shape", *Nuclear Instruments and Methods in Physics Research* A 597, 212–218, 2008.

[17]. M. L. Roush, M. A. Wilson, and W. F. Hornyak, "Pulse shape discrimination", *Nucl. Inst. And Meth. A* 31, 112-124, 1964.

[18]. M. J. Safari, F. D. Abbasi, H. Afarideh, S. Jamili, E. Bayat, "Discrete Fourier Transform Method for Discrimination of Digital Scintillation Pulses in Mixed Neutron-Gamma Fields", *IEEE Trans. Nucl. Sci.* 63(1), 325-332, 2016.